

# Raman Studies of Monolayer Graphene: The Substrate Effect

Ying ying Wang,<sup>†</sup> Zhen hua Ni,<sup>†</sup> Ting Yu,<sup>†</sup> Ze Xiang Shen,<sup>\*,†</sup> Hao min Wang,<sup>‡</sup> Yi hong Wu,<sup>‡</sup> Wei Chen,<sup>§</sup> and Andrew Thye Shen Wee<sup>§</sup>

Division of Physics and Applied Physics, School of Physical & Mathematical Sciences, Nanyang Technological University, Singapore 637371, Department of Electrical and Computer Engineering, National University of Singapore, 4 Engineering Drive 3, Singapore 117576, and Department of Physics, National University of Singapore, 2 Science Drive 3, Singapore, 117542

Received: January 29, 2008; Revised Manuscript Received: April 23, 2008

Graphene has attracted a lot of interest for fundamental studies as well as for potential applications. Till now, micromechanical cleavage (MC) of graphite has been used to produce high-quality graphene sheets on different substrates. Clear understanding of the substrate effect is important for the potential device fabrication of graphene. Here we report the results of the Raman studies of micromechanically cleaved monolayer graphene on standard SiO<sub>2</sub> (300 nm)/Si, single crystal quartz, Si, glass, polydimethylsiloxane (PDMS), and NiFe. Our data suggests that the Raman features of monolayer graphene are independent of the substrate used; in other words, the effect of substrate on the atomic/electronic structures of graphene is negligible for graphene made by MC. On the other hand, epitaxial monolayer graphene (EMG) on SiC substrate is also investigated. Significant blueshift of Raman bands is observed, which is attributed to the interaction of the graphene sheet with the substrate, resulting in the change of lattice constant and also the electronic structure.

## 1. Introduction

Graphene is the two-dimensional (2D) building block for carbon allotropes. Since its first discovery in 2004,<sup>1</sup> graphene has attracted major interest, and there are many ongoing efforts in developing graphene devices because of its high charge mobility and crystal quality.<sup>2–4</sup>

Raman spectroscopy has historically been used to probe structural and electronic characteristics of graphite materials, providing useful information on the defects (D-band), in-plane vibration of sp<sup>2</sup> carbon atoms (G-band), as well as the stacking orders (2D-band).<sup>5</sup> The G-band of graphite materials is a doubly degenerate (TO and LO) phonon mode ( $E_{2g}$  symmetry) at the Brillouin zone center,<sup>6</sup> whereas the D-band is due to phonon branches around the K point and requires a defect for its activation.<sup>5</sup> The evolution of the 2D-band for different graphene sheets has been used for determining graphene thickness as well as for probing electronic structures through the double resonance process.<sup>7,8</sup> The symmetric and sharp 2D-band ( $\sim 30\text{ cm}^{-1}$ ) can be used as a detector for monolayer graphene.<sup>7,8</sup> Even the electron or hole doping can be monitored by Raman measurement, which is reflected in the stiffening and sharpening of the G-band.<sup>9,10</sup>

Till now, most of the Raman studies were carried out on graphene sheets fabricated by micromechanical cleavage (MC) and transferred to Si substrate with appropriate thickness of SiO<sub>2</sub> capping layer ( $\sim 300\text{ nm}$ ).<sup>7,8,11,12</sup> Additionally, there have been studies of graphene on different substrates, such as indium tin oxide (ITO),<sup>13</sup> sapphire, glass,<sup>14</sup> and so on. However, the role of interaction between substrate and the graphene sheets in deciding the Raman features has not been sufficiently investi-

gated, and different conclusions were drawn by different groups. Clear understanding of the substrate effect is important for potential applications and device fabrication of graphene. Therefore, in this work we carry out systematical Raman study of monolayer graphene produced by MC on different substrates: standard SiO<sub>2</sub> (300 nm)/Si, quartz single crystal, Si, glass, PDMS, and NiFe. Choosing monolayer graphene for our study object is first due to the fact that it can be unambiguously identified by Raman spectroscopy from the characteristic 2D-band feature. Second, compared with graphene of a few layers, which are also used to study the substrate effect by other group,<sup>14</sup> monolayer graphene is more sensitive to the interaction between graphene sheets and substrate. We also compared the Raman features of monolayer graphene on the above-mentioned substrates with those of epitaxial monolayer graphene (EMG) grown on SiC substrate, for which we believe there is a much stronger interaction between graphene and substrate. Our experimental results show that the weak interaction (Van de Waals force) between the graphene sheets and substrates prepared by MC are not strong enough to affect the atomic structure of graphene sheets. Only for EMG on SiC substrate do we observe a strong interaction between EMG and SiC, which changes the atomic and electronic structures and consequently the Raman features of graphene.

## 2. Experimental Methods

The graphene samples were prepared by MC<sup>1</sup> and were transferred to different substrates: standard substrate Si wafer with a  $\sim 300\text{ nm}$  SiO<sub>2</sub> capping layer, quartz single crystal, Si, glass, NiFe, and polydimethylsiloxane (PDMS). The EMG samples used in this experiment were epitaxially grown on the *n*-type Si-terminated 6H-SiC (0001) using the technique that has been reported in detail before.<sup>15–18</sup> The thickness of EMG is identified by STM. It is believed that below the EMG there is an interfacial carbon layer/buffer layer that is covalently bonded to the SiC substrate.<sup>19,20</sup> Because the characteristic STM

\* Corresponding author phone: (+65) 6316 8855; fax: (+65) 6794 1325; e-mail: zexiang@ntu.edu.sg.

<sup>†</sup> Nanyang Technological University.

<sup>‡</sup> Department of Electrical and Computer Engineering, National University of Singapore.

<sup>§</sup> Department of Physics, National University of Singapore.

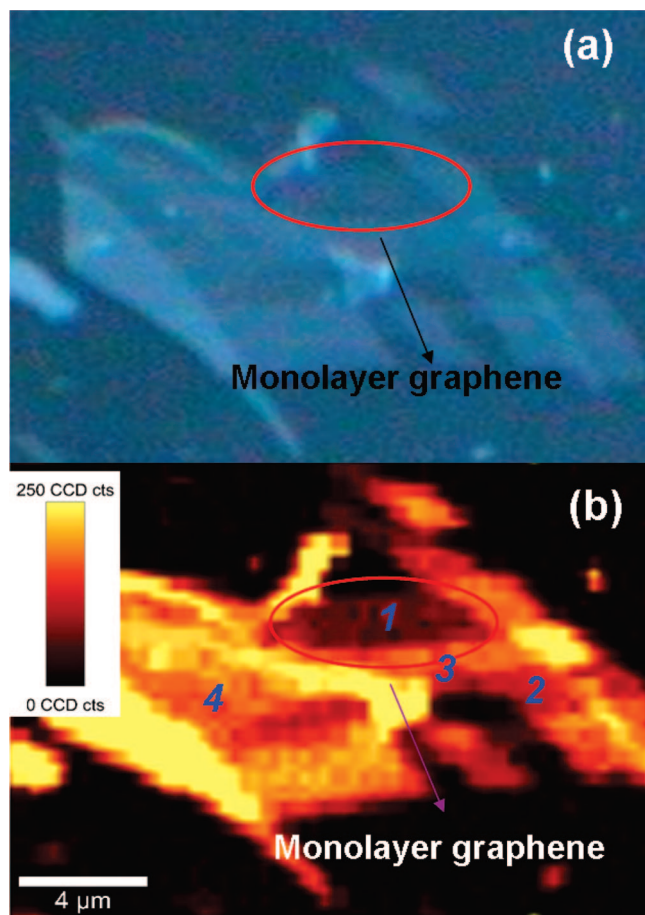


**Figure 1.** (a) Optical image of graphene sheets on quartz, the red circle indicates the location of monolayer graphene. (b) Raman image plotted by the intensity of the G-band. The red circle shows the position of monolayer graphene.

images of the interfacial carbon layer and the single layer graphene are quite different, the appearance of EMG can be determined by monitoring the phase evolution from the interfacial layer to graphene by STM during the thermal annealing of SiC in ultra high vacuum (UHV) condition.<sup>21</sup> The Raman spectra and Raman images were carried out with a WITec CRM200 Raman system with 532 nm (2.33 eV) excitation and laser power at sample below 0.1 mW to avoid laser-induced heating. The laser spot size at focus was around 500 nm in diameter with a 100× optical lens (NA = 0.95). The contrast spectra of graphene were obtained by the following calculation:  $C(\lambda) = (R_0(\lambda) - R(\lambda))/R_0(\lambda)$ , where  $R_0(\lambda)$  is the reflection spectrum from substrate, and  $R(\lambda)$  is the reflection spectrum from graphene sheet, which is illuminated by normal white light.<sup>11</sup> For the contrast and Raman image, the sample was placed on an *x-y* piezostage and scanned under the illumination of laser and white light. The Raman and reflection spectra from every spot of the sample were recorded. The stage movement and data acquisition were controlled using ScanCtrl Spectroscopy Plus software from WITec GmbH, Germany. Data analysis was done using WITec Project software.

### 3. Results and Discussion

Figure 1a shows the optical image of graphene sheets on quartz crystal. The graphene sheets show different contrast regions, which can be understood as having different thickness. The red circle indicates the area of monolayer graphene, which is confirmed by the very sharp 2D-band ( $\sim 30 \text{ cm}^{-1}$ ). A Raman

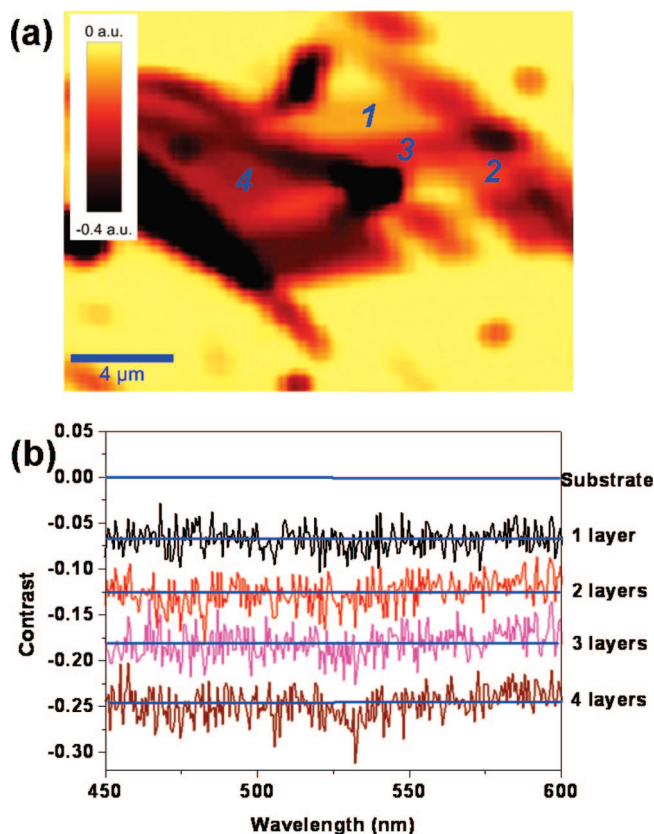


**Figure 2.** (a) The contrast image of graphene sheets on quartz substrate. (b) Contrast spectra of graphene with different thicknesses on quartz substrate.

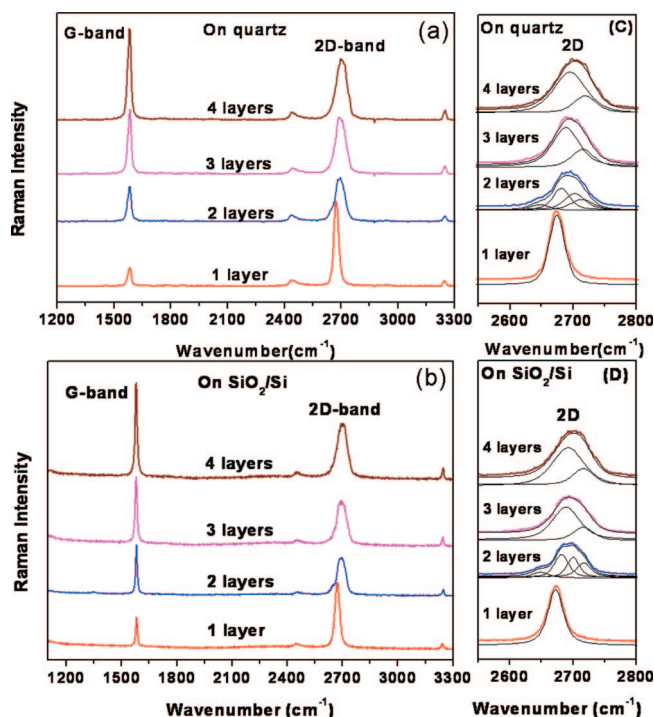


**Figure 3.** The Raman spectra of monolayer, bilayer, three layers, and four layers graphene on quartz (a) and SiO<sub>2</sub> (300 nm)/Si substrate (b). The enlarged 2D-band regions with curve fit are also shown in panels c and d.

image obtained using the intensity of the G-band is shown by Figure 1b. The monolayer graphene has the lowest G-band intensity (appearing the darkest, marked by the red circle). As

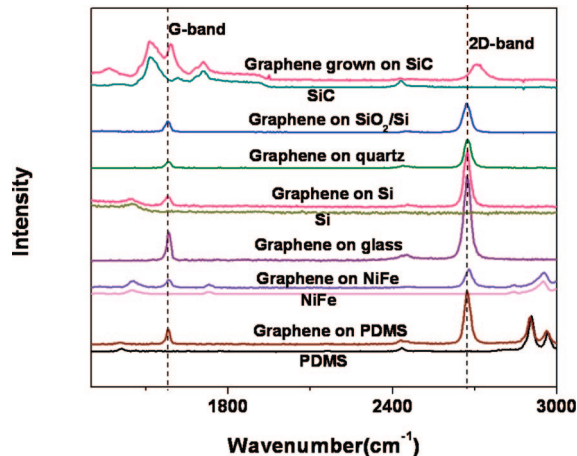


**Figure 4.** The Raman spectra of monolayer graphene on different substrates as well that of epitaxial monolayer graphene on SiC.

the G-band intensity increases almost linearly as the layer increases,<sup>8,11</sup> we are able to identify the thickness of multilayer graphene according to the G-band intensity. The thickness of graphene sheets are further confirmed by reflection and contrast microscopy.<sup>11</sup> The reflection and contrast microscopy was successfully used to determine the number of graphene layers (less than 10) on SiO<sub>2</sub>/Si substrate. The contrast spectra  $C(\lambda)$  are obtained by the calculation shown in eq 1,

$$C(\lambda) = \frac{R_0(\lambda) - R(\lambda)}{R_0(\lambda)} \quad (1)$$

where  $R_0(\lambda)$  is the reflection spectrum from substrate, and  $R(\lambda)$  is the reflection spectrum from graphene sheets. For thin graphene sheets, the contrast value changes almost linearly with the number of layers. Figure 2a shows the contrast image of graphene sheets on quartz substrate. The contrast of graphene is negative because there is more reflection from graphene than quartz. Figure 2b shows the contrast spectra of graphene with different thicknesses. The contrast spectra are almost flat in the range of 450–600 nm and the contrast values are  $-0.068$  (one layer),  $-0.125$  (two layers),  $-0.181$  (three layers), and  $-0.247$  (four layers), which changes almost linearly with the number of layers.

Panels a and b of Figure 3, representively show the Raman spectra of monolayer, bilayer, three layers, and four layers graphene on quartz substrates as well as on the standard SiO<sub>2</sub> (300 nm)/Si substrate for comparison. The Raman features of different layers of graphene on those two substrates are quite

similar. The shape and position of 2D-band change dramatically from one to four layers, as shown in the curve fit of Figure 3, panels c and d. The 2D-band in bilayer, three, and four layers graphene can be resolved into two or more components, whereas monolayer graphene has a single component.<sup>7,8</sup> According to this graph, it can also be seen that the symmetric and sharp 2D-band ( $\sim 30$  cm<sup>-1</sup>) is the best indicator for monolayer graphene made by MC on different substrates.

Figure 4 shows the Raman spectra of monolayer graphene on different substrates, from bottom to top, PDMS, NiFe, glass, Si, quartz, and SiO<sub>2</sub> (300 nm)/Si substrate as well as the Raman spectrum of EMG grown on SiC substrate. The G-band and 2D-band position and their full width at half-maximum (fwhm) for different substrates are summarized in Table I. One can see that G-band position ( $1581 \pm 1$  cm<sup>-1</sup>) and fwhm ( $15.5 \pm 1$  cm<sup>-1</sup>) are similar for graphene on SiO<sub>2</sub> (300 nm)/Si, quartz, Si, glass, NiFe, and PDMS substrates. The small difference in the G-band position on these substrates are within the range of fluctuation ( $1580$ – $1588$  cm<sup>-1</sup>) by unintentional electron or hole doping effect reported by Casiraghi et al.<sup>22</sup> for more than 40 graphene samples on SiO<sub>2</sub>/Si substrate. Therefore, our observation indicates that the interaction between micromechanically cleaved graphene sheets and different substrates is not strong enough to affect the graphene sheets. Our results are in line with Calizo et al.<sup>14</sup> who suggested that the weak substrate effect can be explained by the fact that G-band is made up of the long-wavelength optical phonons (TO and LO),<sup>5</sup> and the out of plane vibrations in graphene are not coupled to this in-plane vibration.<sup>23</sup> On the other hand, for graphene grown on SiC substrate, it can be seen that the intensity ratio of the G- and 2D-bands of EMG differs a lot from those of monolayer graphene made by MC. Moreover, significant blueshifts of the G-band ( $10$  cm<sup>-1</sup>) and the 2D-band ( $\sim 39$  cm<sup>-1</sup>) of EMG are observed compared to those of graphene made by MC. There might be some electron doping transferred from the underlying SiC to EMG (due to the covalent bonding),<sup>24,25</sup> however it should not be the main reason for Raman blueshift. It is shown that the dependence of doping on shift in the 2D-band is very weak and is roughly  $\sim 10$ – $30\%$  compared to that of G-band;<sup>9,26,27</sup> therefore, the  $39$  cm<sup>-1</sup> 2D-band shift is too large to be achieved by electron/hole dopings.<sup>9,10</sup> Here, this significant blueshift of Raman bands can be understood by the strain effect caused by the substrate. Between EMG and the SiC substrate, there is an interfacial carbon layer/buffer layer, which has a graphene-like honeycomb lattice that is covalently bonded to the SiC substrate.<sup>19,20</sup> Such bonding would change its lattice constant as well as the electronic properties. Therefore, the lattice

**TABLE I: The G-band and 2D-band Position and Their fwhm for Graphene/Graphite on Different Substrates<sup>a</sup>**

substrate	G-band position (cm <sup>-1</sup> )	G-band fwhm (cm <sup>-1</sup> )	2D-band position (cm <sup>-1</sup> )	2D-band fwhm (cm <sup>-1</sup> )
SiC	1591.5	31.3	2710.5	59.0
SiO <sub>2</sub> /Si	1580.8	14.2	2676.2	31.8
SiO <sub>2</sub> /Si <sup>22</sup>	1580–1588	6–16		
Quartz	1581.9	15.6	2674.6	29.0
Si	1580	16	2672	28.3
PDMS	1581.6	15.6	2673.6	27
Glass	1582.5	16.8	2672.8	30.8
Glass <sup>14</sup>	1580	35 (split)		
NiFe	1582.5	14.9	2678.6	31.4
GaAs <sup>14</sup>	1580	15		
Sapphire <sup>14</sup>	1575	20		
Graphite	1580.8	16.0	2D1: 2675.4 2D2: 2720.8	41.4 35.6

<sup>a</sup> Results from refs 14 and 22 are also included.

mismatch between graphene lattice and interfacial carbon layer may cause a compressive stress on EMG, hence the shift of the G-band Raman peak frequencies.<sup>21</sup>

Graphene on different substrates such as ITO,<sup>13</sup> sapphire, and glass<sup>14</sup> have also been investigated by other groups. In contrast to their results, we did not observe the split or large red/blue shift of the Raman G-band of graphene on different substrates made by MC,<sup>14</sup> partially due to the different starting materials or preparing methods used. The possibility of forming bonds between micromechanically cleaved graphene and substrate is quite low as such bonds are only possible at high-temperature growth.<sup>24,25,28</sup>

#### 4. Conclusions

In summary, through our Raman studies of monolayer graphene produced by MC on different substrates—standard SiO<sub>2</sub> (300 nm)/Si, quartz, Si, glass, NiFe, and PDMS—we could know the weak interaction (Van de Waals force) between graphene sheets and the substrates play a negligible role in affecting the Raman features of graphene sheets. Only EMG grown on SiC substrate shows strong blueshift of G-band, which can be understood by the strain effect caused by the covalent bonding between SiC substrate and epitaxial graphene, resulting in the changes the lattice constant of graphene, and hence the Raman features.

#### References and Notes

- (1) Novoselov, K. S.; Geim, A. K.; Morozov, S. V.; Jiang, D.; Zhang, Y.; Dubonos, S. V.; Grigorieva, I. V.; Firsov, A. A. *Science*, **2004**, *306*, 666.
- (2) Novoselov, K. S.; Geim, A. K.; Morozov, S. V.; Jiang, D.; Katsnelson, M. I.; Grigorieva, I. V.; Dubonos, S. V.; Firsov, A. A. *Nature*, **2005**, *438*, 197.
- (3) Zhang, Y. B.; Tan, Y. W.; Stormer, H. L.; Kim, P. *Nature* **2005**, *438*, 201.
- (4) Novoselov, K. S.; Jiang, Z.; Zhang, Y.; Morozov, S. V.; Stormer, H. L.; Zeitler, U.; Maan, J. C.; Boebinger, G. S.; Kim, P.; Geim, A. K. *Science* **2007**, *315*, 1379.
- (5) Pimenta, M. A.; Dresselhaus, G.; Dresselhaus, M. S.; Cancado, L. G.; Jorio, A.; Saito, R. *Phys. Chem. Chem. Phys.* **2007**, *9*, 1276.
- (6) Tuinstra, F.; Koenig, J. L. *J. Chem. Phys.* **1970**, *53*, 1126.

- (7) Ferrari, A. C.; Meyer, J. C.; Scardaci, V.; Casiraghi, C.; Lazzeri, M.; Mauri, F.; Piscanec, S.; Jiang, D.; Novoselov, K. S.; Roth, S.; Geim, A. K. *Phys. Rev. Lett.* **2006**, *97*, 187401.
- (8) Graf, D.; Molitor, F.; Ensslin, K.; Stampfer, C.; Jungen, A.; Hierold, C.; Wirtz, L. *Nano Lett.* **2007**, *7*, 238.
- (9) Yan, J.; Zhang, Y. B.; Kim, P.; Pinczuk, A. *Phys. Rev. Lett.* **2007**, *98*, 166802.
- (10) Pisana, S.; Lazzeri, M.; Casiraghi, C.; Novoselov, K. S.; Geim, A. K.; Ferrari, A. C.; Mauri, F. *Nat. Mater.* **2007**, *6*, 198.
- (11) Ni, Z. H.; Wang, H. M.; Kasim, J.; Fan, H. M.; Yu, T.; Wu, Y. H.; Feng, Y. P.; Shen, Z. X. *Nano Lett.* **2007**, *7*, 2758.
- (12) Casiraghi, C.; Hartschuh, A.; Lidorikis, E.; Qian, H.; Harutyunyan, H.; Gokus, T.; Novoselov, K. S.; Ferrari, A. C. *Nano Lett.* **2007**, *7*, 2711.
- (13) Das, A.; Chakraborty, B.; Sood, A. K. *arXiv*: 0710.4160.
- (14) Calizo, I.; Bao, W. Z.; Miao, F.; Ning Lau, C.; Balandin, A. A. *Appl. Phys. Lett.* **2007**, *91*, 201904.
- (15) Berger, C.; Song, Z. M.; Li, X. B.; Wu, X. S.; Brown, N.; Naud, C.; Mayo, D.; Li, T. B.; Hass, J.; Marchenkov, A. N.; Conrad, E. H.; First, P. N.; De Heer, W. A. *Science* **2006**, *312*, 1191.
- (16) Berger, C.; Song, Z. M.; Li, X. B.; Ogbazghi, A. Y.; Feng, R.; Dai, Z. T.; Marchenkov, A. N.; Conrad, E. H.; First, P. N.; de Heer, W. A. *J. Phys. Chem. B* **2004**, *108*, 19912.
- (17) Chen, W.; Chen, S.; Qi, D. C.; Gao, X. Y.; Wee, A. T. S. *J. Am. Chem. Soc.* **2007**, *129*, 10418.
- (18) Chen, W.; Xu, H.; Liu, L.; Gao, X. Y.; Qi, D. C.; Peng, G. W.; Tan, S. C.; Feng, Y. P.; Loh, K. P.; Wee, A. T. S. *Surf. Sci.* **2005**, *596*, 176.
- (19) Emtsev, K. V.; Speck, F.; Seyller, Th.; Ley, L.; Riley, J. D. *Phys. Rev. B* **2008**, *77*, 155303.
- (20) Varchon, F.; Feng, R.; Hass, J.; Li, X.; Ngoc Nguyen, B.; Naud, C.; Mallet, P.; Veuillen, J.-Y.; Berger, C.; Conrad, E. H.; Magaud, L. *Phys. Rev. Lett.* **2007**, *99*, 126805.
- (21) Ni, Z. H.; Chen, W.; Fan, X. F.; Kuo, J. L.; Yu, T.; Wee, A. T. S.; Shen, Z. X. *Phys. Rev. B* **2008**, *77*, 115416.
- (22) Casiraghi, C.; Pisana, S.; Novoselov, K. S.; Geim, A. K.; Ferrari, A. C. *Appl. Phys. Lett.* **2007**, *91*, 233108.
- (23) Falkovsky, L. A. *J. Exp. Theor. Phys.* **2007**, *105*, 397.
- (24) Zhou, S. Y.; Gweon, G. -H.; Fedorov, A. V.; First, P. N.; de Heer, W. A.; Lee, D. H.; Guinea, F.; Neto, A. H. C.; Lanzara, A. *Nat. Mater.* **2007**, *6*, 770.
- (25) Ohta, T.; Bostwick, A.; Seyller, T.; Horn, K.; Rotenberg, E. *Science* **2006**, *313*, 951.
- (26) Das, A.; Pisana, S.; Piscanec, S.; Chakraborty, B.; Saha, S. K.; Waghmare, U. V.; Novoselov, K. S.; Krishnamurthy, H. R.; Geim, A. K.; Ferrari, A. C.; Sood, A. K. *Nat. Nanotechnol.* **2008**, *3*, 210.
- (27) Stampfer, C.; Molitor, F.; Graf, D.; Ensslin, K.; Jungen, A.; Hierold, C.; Wirtz, L. *Appl. Phys. Lett.* **2007**, *91*, 241907.
- (28) Han, S.; Liu, X.; Zhou, C. *J. Am. Chem. Soc.* **2005**, *127*, 5294.

JP8008404